

Article

Heatwave Effects on the Photosynthesis and Antioxidant Activity of the Seagrass *Cymodocea nodosa* under Contrasting Light Regimes

Monya M. Costa, João Silva *, Isabel Barrote [†] and Rui Santos [†]

Centre of Marine Sciences (CCMAR), University of Algarve, Campus Gambelas, 8005-139 Faro, Portugal; mmcosta@ualg.pt (M.M.C.); ibarrote@ualg.pt (I.B.); rosantos@ualg.pt (R.S.)

* Correspondence: jmsilva@ualg.pt; Tel.: +35-12898-00051

[†] These authors contributed equally to this work.

Abstract: Global climate change, specifically the intensification of marine heatwaves, affect seagrasses. In the Ria Formosa, saturating light intensities may aggravate heatwave effects on seagrasses, particularly during low spring tides. However, the photophysiological and antioxidant responses of seagrasses to such extreme events are poorly known. Here, we evaluated the responses of *Cymodocea nodosa* exposed at 20 °C and 40 °C and 150 and 450 $\mu\text{mol quanta m}^{-2} \text{s}^{-1}$. After four-days, we analyzed (a) photosynthetic responses to irradiance, maximum photochemical efficiency (Fv/Fm), the effective quantum yield of photosystem II (ϕPSII); (b) soluble sugars and starch; (c) photosynthetic pigments; (d) antioxidant responses (ascorbate peroxidase, APX; oxygen radical absorbance capacity, ORAC, and antioxidant capacity, TEAC); (d) oxidative damage (malondialdehyde, MDA). After four days at 40 °C, *C. nodosa* showed relevant changes in photosynthetic pigments, independent of light intensity. Increased TEAC and APX indicated an “investment” in the control of reactive oxygen species levels. Dark respiration and starch concentration increased, but soluble sugar concentrations were not affected, suggesting higher CO₂ assimilation. Our results show that *C. nodosa* adjusts its photophysiological processes to successfully handle thermal stress, even under saturating light, and draws a promising perspective for *C. nodosa* resilience under climate change scenarios.

Keywords: seagrasses; antioxidant response; heat waves; high temperature; *Cymodocea nodosa*; oxidative stress



Citation: Costa, M.M.; Silva, J.; Barrote, I.; Santos, R. Heatwave Effects on the Photosynthesis and Antioxidant Activity of the Seagrass *Cymodocea nodosa* under Contrasting Light Regimes. *Oceans* **2021**, *2*, 448–460. <https://doi.org/10.3390/oceans2030025>

Academic Editor: Bernardo Duarte

Received: 10 March 2021

Accepted: 15 June 2021

Published: 25 June 2021

Publisher's Note: MDPI stays neutral with regard to jurisdictional claims in published maps and institutional affiliations.



Copyright: © 2021 by the authors. Licensee MDPI, Basel, Switzerland. This article is an open access article distributed under the terms and conditions of the Creative Commons Attribution (CC BY) license (<https://creativecommons.org/licenses/by/4.0/>).

1. Introduction

Seagrass meadows are among the most productive ecosystems on earth and deliver significant ecosystem services in shallow marine habitats. Despite their relevance, seagrasses are under threat [1,2], with wide losses being attributed to disease [3], anthropogenic impacts [1], and to the increased frequency of extreme climatic events, such as marine heatwaves (MHW) [4–7]. MHW are generally defined as transient periods of extremely warm water, where the temperature exceeds the 90th percentile of a 30-year baseline database [8]. Marine heatwaves put seagrass growth and survival at risk and affect their distribution with subsequent impacts on the associated habitats [7].

Temperature is a key factor, affecting enzyme activity and metabolism of marine organisms [9], which, according to the species-specific tolerance, may be translated to an imbalance in photosynthesis and respiration. Reported effects of high temperatures (HT) on seagrasses include changes in photosynthesis [10] and respiration [11]. Inhibition or decrease of photosynthesis and increase in respiration due to HT or MHW was described in *Z. marina* [9], *Thalassia hemprichii*, *Enhalus acoroides* [11], and *P. oceanica* [12]. The negative impact of high temperature on chlorophyll fluorescence, indicating damage or inactivation of the photosynthetic apparatus, was observed in *Z. marina* and *T. hemprichii* [13]. In addition, high temperature can also induce changes in seagrass cell membranes [10], photosynthetic pigments (chlorophyll a and chlorophyll b), and strong oxidative damage [14].

Cymodocea nodosa is a warm-temperate species, naturally adapted to medium-high temperatures (25–32 °C) [12,15], which distribution in the Mediterranean and been predicted by niche models to be reduced by 46.5% under global warming [16]. This species has been described as tolerant to high temperatures, with the potential to survive MHW considering its photosynthetic responses, gene expression [12,17], increase in gross primary production [16], and higher optimal temperature for growth when compared to other species of the same community [18]. Still, Koutalianou et al. [19] observed potential cellular damage and cytoskeleton disturbances in *C. nodosa* under high temperature, (38 °C) and, according to [17], physiological processes can be negatively affected by temperatures above *C. nodosa* critical thresholds, with impacts in species survival and habitat degradation [16].

Moreover, high light levels may be stressful to seagrasses, again with species-specific responses, and affect several metabolic processes, such as electron transport rate [20], carbon acquisition, and fixation [21]. *Thalassia hemprichii* is less responsive to high light than *Halophila ovalis* [22], in which the photoprotective mechanisms involve increased dissipation of excess energy and the activity of antioxidant enzymes. Schubert et al. [23] found anatomic modifications in seagrass leaves in response to light availability, more pronounced in *C. nodosa* than in *Zostera marina* and *Zostera noltii*. Co-occurring stressors, such as high-temperatures, condition the plants' light use capacity by affecting several metabolic processes, such as electron transport rate [20], carbon acquisition, and fixation [21].

In tidal regimes, especially in shallow habitats, seagrasses can often be submitted to a combination of high temperatures and high irradiance, particularly during low tides [24]. The combined effects of light and temperature are known to have the potential to magnify stress reactions when compared with isolated effects [25]. George et al. [24] found a stronger effect of temperature stress on four tropical seagrasses when it occurred during solar noon. In the Ria Formosa lagoon, shifts of >10 °C in water temperature are common in the span of just a few hours, with peaks of temperature coinciding with the highest light levels, namely when low tide occurs at midday [26]. *C. nodosa* can thus be simultaneously exposed to light levels above the saturating irradiance, which become potentially photo-damaging when co-occurring with extreme temperatures. These events tend to be more pronounced in the future, with the expected increase of the intensity, frequency, and duration of heatwaves ([27] and references therein).

This study aims to assess the effects of a simulated marine heatwave on the high-temperature tolerant species *C. nodosa* under contrasting light regimes. Specifically, the antioxidant response and the impact on plant photo-physiology (photosynthesis, photosynthetic pigments, and photosynthetic products, such as soluble sugars) of the simulated heatwave were evaluated. Furthermore, the putative synergistic highlight plus high-temperature effect was investigated.

2. Materials and Methods

2.1. Site Description

In the Ria Formosa lagoon, southern Portugal (37° N, 008° W), *Cymodocea nodosa* is abundant in the shallow subtidal, where physiologically demanding conditions may occur, particularly in the summer during low spring tides, when the plants are confined to relatively small ponds where water temperature and light reach very high values. *C. nodosa* plants were collected in May and June 2011, when seawater temperature ranged between 18 °C and 30 °C (<https://www.hidrografico.pt/boias>, accessed on 30 May 2011), and light at the canopy level ranged between 230 and 400 $\mu\text{mol quanta m}^{-2} \text{s}^{-1}$ (Li-192SA underwater quantum sensor connected to Li-1000 data logger; Li-Cor).

2.2. Experimental Design

C. nodosa plants, including rhizomes and roots, with the apical meristem, and three or more shoots with 3–4 leaves each, were harvested from the middle of a large meadow and immediately replanted in glass aquaria (9.5 × 15 × 7.5 cm, 23 shoots each), using sterilized fine sand (pore size < 2 mm) as substrate to cover the rhizomes (ca 2–4 cm depth).

Three independent aquaria were used as replicates for each treatment ($n = 3$). Aquaria were filled with natural seawater that was continuously aerated and renewed every 48 h. Prior to renewal, seawater temperature was brought to the experimental level for 24 h. The experiment was run in a walk-in growth chamber, with incorporated temperature control (Aralab 1000 Thin), in a factorial four-day set-up of water temperature (20 °C and 40 °C) and light (150 and 450 $\mu\text{mol quanta m}^{-2} \text{s}^{-1}$), provided by OSRAM Powerstar HOI-BT 400W/D Daylight lamps, in combination with 100W Halolux Ceram lamps) with a photoperiod of 12 h:12 h. The lower light level was obtained by covering the aquaria with neutral greenhouse shading nets. The temperature was monitored continuously with a HOBO temperature logger, and light intensity inside the leaf canopy was checked daily with a Li-192SA underwater quantum sensor connected to a Li-1000 data logger (Li-Cor). The choice of an extreme heatwave temperature of 40 °C was selected based on temperatures previously measured by the authors in the water ponds formed during low spring tides in the Ria Formosa; 40 °C is 5 °C higher than the highest temperatures measured. The higher light intensity was selected to saturate for *C. nodosa* (minimum saturation irradiance: $397.68 \pm 40.08 \mu\text{mol quanta m}^{-2} \text{s}^{-1}$, [28]).

2.3. Photosynthesis and Dark Respiration

Photosynthesis-irradiance (P-I) curves ($n = 3$) were determined at the experimental temperatures with an oxygen electrode (DW3/CB1, Hansatech, Norfolk, UK) according to Silva et al. [29]. Briefly, the middle part of the second or third leaf (mature leaves) of each replicate was mounted vertically inside the measuring chamber, for an even exposure to the different incident light intensities. Dark respiration was measured using the same procedure in the dark. Data points that deviated from the upper and lower quartiles more than 1.5-fold the interquartile range were considered outliers and, thus, were not included in the analysis [30]. P-I curves were fitted with the mathematical model equation by Jassby and Plat [31].

Both the maximum quantum efficiency of photosystem II photochemistry (F_v/F_m) and the effective quantum yield of photochemical energy conversion in PSII (ϕ_{PSII}) were measured at the end of the experiment (four days), using a pulse amplitude modulated fluorometer (Diving-PAM, Heinz Walz, Effeltrich, Germany). For F_v/F_m measurements, plants were dark-adapted for 30 min prior to fluorescence measurements.

2.4. Biochemical Analysis

To avoid the influence of tissue age on the responses to temperature and light [29,32], only the middle parts of the second and third leaf of each shoot of *C. nodosa* (excluding the apex and the meristem) were used for biochemical analysis. *C. nodosa* leaf samples were collected and prepared as described in [33]. Briefly, the samples were cleaned of epiphytes, rinsed with distilled water, blotted dry and immediately frozen in liquid nitrogen, and stored at $-80 \text{ }^\circ\text{C}$ until analysis. The whole procedure took about 5 min per sample. Leaf sampling was completely performed inside the walk-in growth chamber at the experimental light and temperature conditions.

2.4.1. Antioxidant Responses

The methods used to evaluate the antioxidant scavenging capacity can be divided in two groups [34]: assays that quantify the protection capacity against peroxy radicals ($\text{ROO}\bullet$) through hydrogen atom transfer (HAT) and assays that quantify the total antioxidant capacity based on a single electron transfer (ET). Here we assessed the global antioxidant capacity of the seagrass *C. nodosa* using both types of assay, respectively oxygen reactive absorbance capacity (ORAC) and trolox equivalent antioxidant capacity (TEAC). ORAC quantifies the antioxidant capacity of phenolic compounds and tocopherols. It has been extensively used by pharmaceutical, nutritional and food industries to determine total antioxidant capacity [35]. TEAC quantifies the antioxidant activity related with carotenoids, phenolic compounds, superoxide dismutase, ascorbate peroxidase, and

reducing agents such as ascorbate, glutathione, and NADPH. It has been widely used to determine the antioxidant capacity of terrestrial plants [36,37]. The extraction for ORAC and TEAC quantification was performed simultaneously. Frozen leaf samples (300 mg, $n = 3$), were powdered in liquid nitrogen, suspended in 0.1 N hydrochloric acid (HCl), and kept overnight under constant agitation at 4 °C followed by centrifugation at $4700 \times g$ for 30 min. Quantifications were performed on the supernatant.

ORAC was quantified according to [35]: 75 mM phosphate buffer and 8.16×10^{-5} mM fluorescein (Sigma) were added to the extract and this mixture was heated to 37 °C and read in a Synergy TM 4 multi-detection microplate reader with a 485 nm, 20 nm bandpass, excitation filter and a 528 nm, 20 nm bandpass, emission filter. The reaction was initiated by the addition of 153 mM ABAP (2,2'-azobis (2-methylpropionamidine) dihydrochloride) (Sigma). Results were expressed as Trolox[®] equivalents (6-hydroxy-2,5,7,8-tetramethylchromane-2-carboxylic acid).

For TEAC quantification, ABTS^{•+} (radical monocation of 2,2'-azinobis-(3-ethylbenzothiazoline-6-sulphonic acid) was produced by the reaction of 7 mM ABTS with potassium persulfate in a final concentration of 2.45 mM [38]. Diluted ABTS^{•+} ($A_{734\text{nm}} = 0.800 \pm 0.020$) was added to the extract and, after a 6 min incubation period, absorbance was read at 734 nm in a Beckman Coulter DU-650 spectrophotometer. Results were expressed as Trolox[®] equivalents (6-hydroxy-2,5,7,8-tetramethylchromane-2-carboxylic acid).

To assess the ascorbate peroxidase (APX) activity, frozen leaf tissue (800 mg, $n = 3$) was powdered in liquid nitrogen with polyvinylpyrrolidone (PVPP) and sodium ascorbate and then extracted in 5 mL of 100 mM potassium phosphate buffer (pH 7.8) with 2% triton-x and 10 mM ascorbate. Extracts were centrifuged at 4 °C, $3500 \times g$ for 30 min. Supernatants were purified by filtration with Sephadex PD-10 G-25 columns (GE Healthcare) [39], previously equilibrated with 20 mL of 100 mM potassium phosphate buffer (pH 7.0) with 1 mM ascorbate. APX activity was measured at 25 °C, by following for 3 min the decrease in absorbance at 290 nm of a mixture containing 50 mM potassium phosphate buffer (pH 7.0), 8 mM ascorbate, and 20 mM hydrogen peroxide (adapted from [40]). APX activity was calculated after subtraction of the control rates, where the enzyme extract was replaced by the potassium phosphate buffer, using $\epsilon = 2.8 \text{ mM}^{-1} \text{ cm}^{-1}$. One unit (U) of APX is equivalent to the protein necessary to oxidize one μmol of ascorbate per minute. Enzyme activity was expressed in U mg^{-1} of leaf dry weight (DW).

To evaluate oxidative damage, malondialdehyde (MDA) was quantified. Lipids are a major component of cell membranes, and the breakdown products of membrane fatty acid peroxides, such as MDA, are commonly used as reliable markers of oxidative stress [41].

MDA quantification was performed according to [42]. Frozen leaf tissue (300 mg, $n = 3$) was powdered in liquid nitrogen, suspended in 80% aqueous ethanol and then centrifuged at $3000 \times g$ for 10 min. The supernatant was added to a solution of 20% trichloroacetic acid (TCA) with 0.65% thiobarbituric acid (TBA) and 0.015% butylated hydroxytoluene (BHT). Two blanks were performed, either without TBA or with 80% ethanol instead of sample extract. All samples and blank reaction mixtures were incubated at 90 °C for 25 min., then cooled for 15 min and again centrifuged. Absorbance of the supernatants were read at 440, 532, and 600 nm in a Beckman Coulter DU-650 spectrophotometer, and MDA equivalents were calculated as in [42].

2.4.2. Photosynthetic Pigments

Frozen leaf tissue (200 mg, $n = 3$) was powdered in liquid nitrogen and sodium ascorbate, and photosynthetic pigments were extracted under dim light in 5 mL of acetone 100% and NaHCO_3 [43]. Extracts were filtered sequentially with 5.0 μm LS membrane and PTFE 0.2 μm hydrophobic filters. Chlorophylls *a* and *b* were quantified spectrophotometrically, using the equations of [44], while carotenoids were analyzed by isocratic high performance liquid chromatography (HPLC) as in [45] after [46].

HPLC analysis of extracts and standards (20 μL) were carried out in an Alliance Waters 2695 separation module, with a Waters 2996 photodiode array detector and a Waters

Novapak C18 radial 8×100 mm compression column ($4 \mu\text{m}$ particle size). During injection, extracts were maintained at 5°C . The mobile phase was pumped at a 1.7 mL flow. The mobile phase A, acetonitrile:methanol:triethylamine (7.5:1:0.7), was fluxed through the column, in an isocratic 3.5 min step, followed by mobile phase B, acetonitrile:methanol:mili-q water:ethyl acetate (7:0.96:0.04:8) in a 6.5 min isocratic step. Between injections, the column was equilibrated with mobile phase A for 5 min. All eluents were prepared with HPLC grade solvents (VWR HiPerSolv Chromanorm), filtered, and sonicated prior to use. During all chromatographic analysis, the column was kept at a steady temperature (24°C). Calibration was done with commercially available pigments (CaroteNature, Lupsingen, Switzerland). Peak areas were monitored at 450 nm . Pigment concentrations were calculated based on peak areas from standards in known concentrations. For calibration curves, all standard dilutions were injected eight times for each pigment. The de-epoxidation state (DES) of the xanthophyll cycle pigments was calculated as $(A+Z)/(V+A+Z)$ [47,48], where A stands for antheraxanthin, Z for zeaxanthin, and V for violaxanthin.

2.4.3. Soluble Sugars and Starch

Freeze-dried leaf tissue (10 mg , $n = 3$) was ground to powder, in a ball mill (RETSCH, MM 300, extracted with ethanol 80% for 10 min at 80°C and centrifuged at $2000 \times g$ 5 min (adapted from [49]). The supernatant was collected, and the pellet resuspended in ethanol for an additional extraction. This procedure was repeated three consecutive times. The supernatants from the three-step extraction were combined and used for soluble sugars quantification by phenol-sulfuric method [50]. Calibration was performed using glucose as standard.

For starch quantification, the pellet from soluble sugars extraction was washed 3 times with distilled water, resuspended in 1 mL of distilled water, and incubated for 10 min at 100°C . Starch was hydrolyzed by a 24 h incubation in an enzymatic solution with 1000 U/mg α -amylase and 14 U/mL amyloglucosidase. After hydrolysis, starch was quantified in the extracts as glucose equivalents as described for soluble sugars.

2.5. Data Analysis

All results are presented as mean \pm standard error. The effects of temperature (20°C , 40°C) and light (150 and $450 \mu\text{mol quanta m}^{-2} \text{ s}^{-1}$) on the variables measured were tested using Two-way analyses of variance (ANOVA) after checking parametric assumptions. The Student–Newman–Keuls post-hoc test was used for significant differences between factor levels. All data treatment and statistical analysis were performed using Sigma Stat/SigmaPlot (SPSS Inc., v. 11) software package.

3. Results

3.1. Photosynthesis and Dark Respiration

Both the maximum quantum efficiency (F_v/F_m) and the effective quantum yield of photochemical energy conversion in PSII (ϕPSII) decreased significantly with light (Figure 1a,b). As opposed to F_v/F_m , ϕPSII increased with temperature (Figure 1a,b).

Maximum photosynthesis (P_{max}) (Figure 1c) was higher at 20°C than at 40°C , independently of light. Although, P_{max} was not affected by light, at 40°C and $450 \mu\text{mol quanta m}^{-2} \text{ s}^{-1}$, P-I results were to disperse and did not allow de mathematical adjustment of the curve.

Dark respiration increased 3.95-fold with temperature (Figure 1d), and although it was not significantly affected by light, at 20°C and $450 \mu\text{mol quanta m}^{-2} \text{ s}^{-1}$, dark respiration was lower than at $150 \mu\text{mol quanta m}^{-2} \text{ s}^{-1}$.

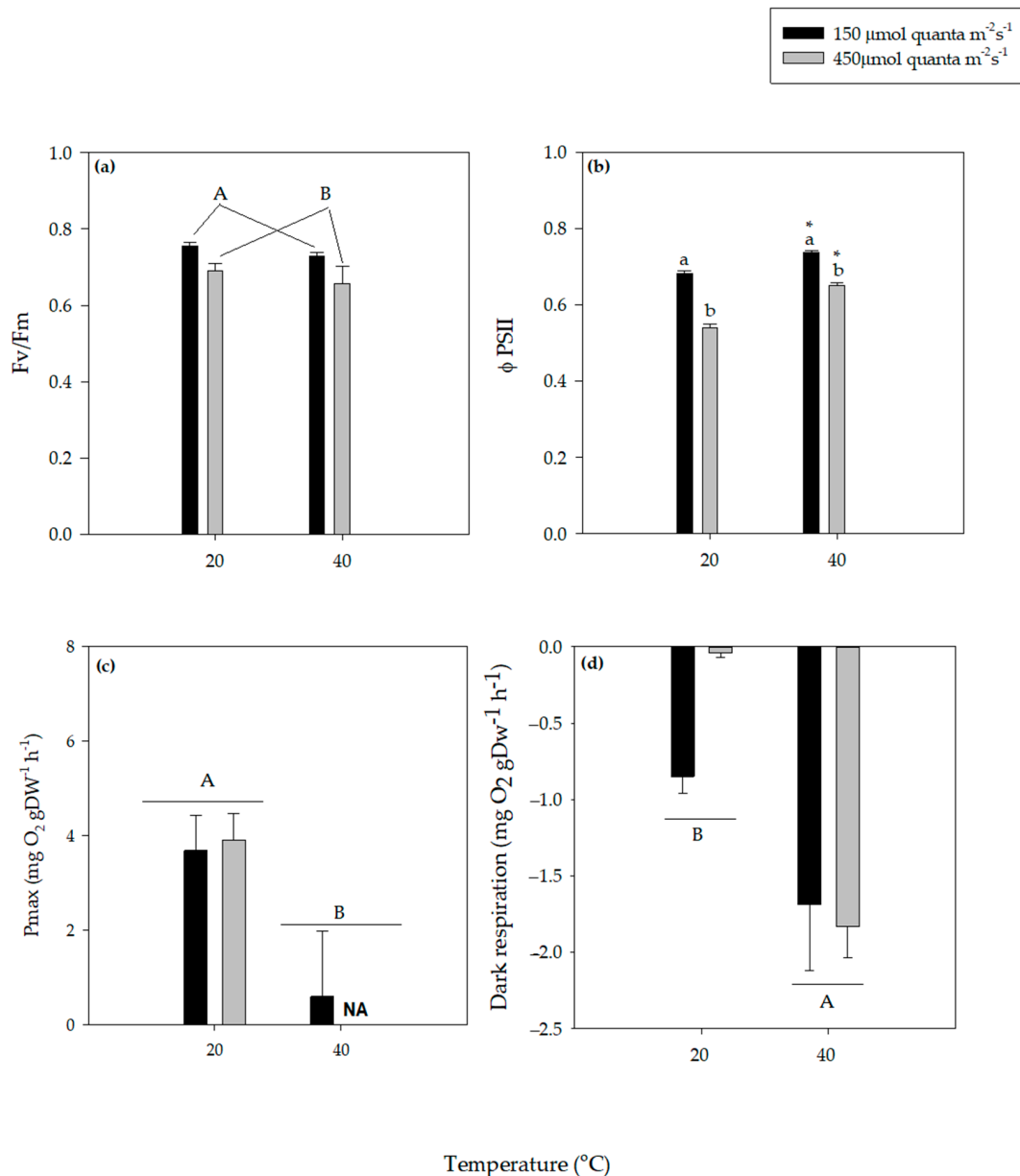


Figure 1. Effects of temperature and light on *Cymodocea nodosa*: (a) PSII maximal photochemical efficiency (Fv/Fm); (b) effective quantum yield of photochemical energy conversion in PSII (ϕ PSII); (c) Maximum photosynthesis (Pmax), NA—the dispersion of the points under this condition did not allow the adjustment to calculate the parameters; (d) and dark respiration. Values represent mean \pm SE ($n = 3$). Different letters indicate significant differences among light levels under the same temperature ($p < 0.05$, SNK test); * indicate significant differences among temperatures under the same light level ($p < 0.05$, SNK test); capital letters indicate differences among temperature or light independently of the other factor (no interaction among factors; $p < 0.05$, SNK test).

3.2. Antioxidant Responses

The experimental heatwave of 40 °C increased both the antioxidant activity quantified by TEAC (Figure 2a) and of the APX activity (Figure 2b). APX activity was 1.4-fold higher in leaves at 40 °C than at 20 °C. ORAC was not affected by temperature (Figure 2c) and none of the antioxidant responses tested were affected by light (Figure 2).

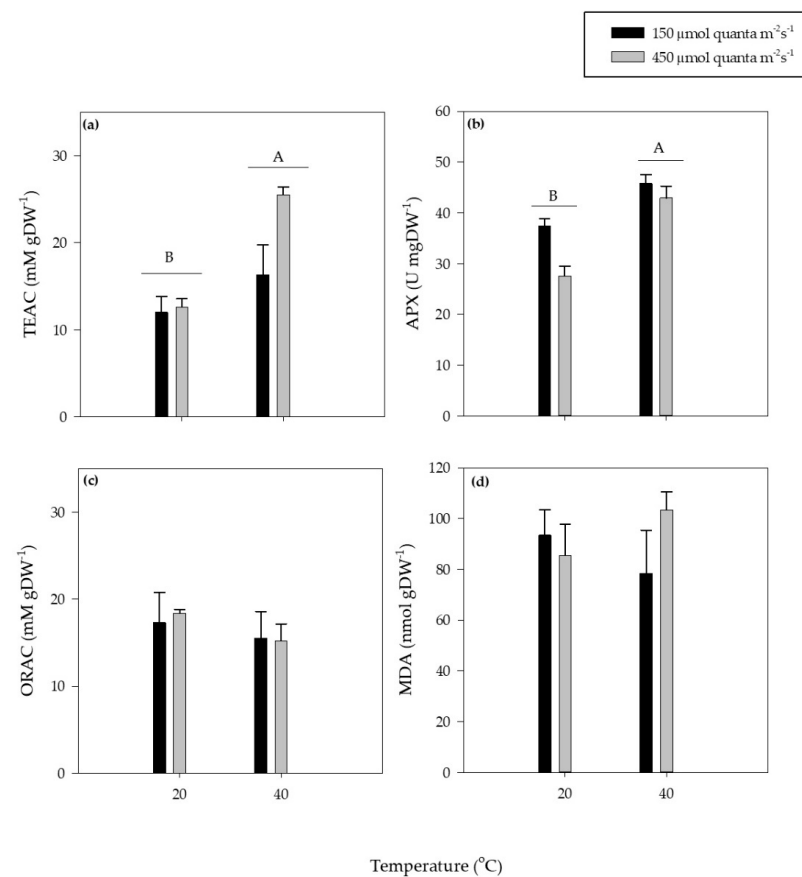


Figure 2. Effects of temperature and light on *Cymodocea nodosa*: (a) trolox equivalent antioxidant capacity (TEAC); (b) ascorbate peroxidase (APX) activity; (c) reactive oxygen species absorbance capacity (ORAC); and (d) malondialdehyde (MDA) concentration. Values represent mean \pm SE ($n = 3$). Different letters indicate significant differences among light levels under the same temperature ($p < 0.05$, SNK test); * indicate significant differences among temperatures under the same light level ($p < 0.05$, SNK test); capital letters indicate differences among temperature independently of light level (no interaction among factors; $p < 0.05$, SNK test).

The increase in light or temperature did not cause oxidative damage, as measured by malondialdehyde MDA (Figure 2d).

3.3. Photosynthetic Pigments

Significant changes occurred in the balance between carotenoids and chlorophylls in response to the higher temperature (40 °C) where, in general, carotenoids content decreased relatively to chlorophyll due to the significant increase in leaf total chlorophyll content (Supplementary Materials Table S1).

Foliar chlorophyll *b* concentration was higher under 40 °C no matter the light intensity, as opposed to chlorophyll *a* that was not affected by temperature and light intensity (Supplementary Materials Table S1). In addition, higher chlorophyll *b* at 40 °C resulted in significantly higher total chlorophyll (Supplementary Materials Table S1).

There were no changes in total carotenoid foliar content with temperature or light (Supplementary Materials Table S1). Additionally, the sum of the pigments of the xanthophyll cycle, violaxanthin (V), antheraxanthin (A) zeaxanthin (Z) did not change with light or temperature (Supplementary Materials Table S1). However, the de-epoxidation index (DES) decreased under high temperature, but this decrease was only significant under low light (150 $\mu\text{mol quanta m}^{-2} \text{s}^{-1}$) (Figure 3a). As expected, DES was higher under the higher irradiance at both the temperatures tested.

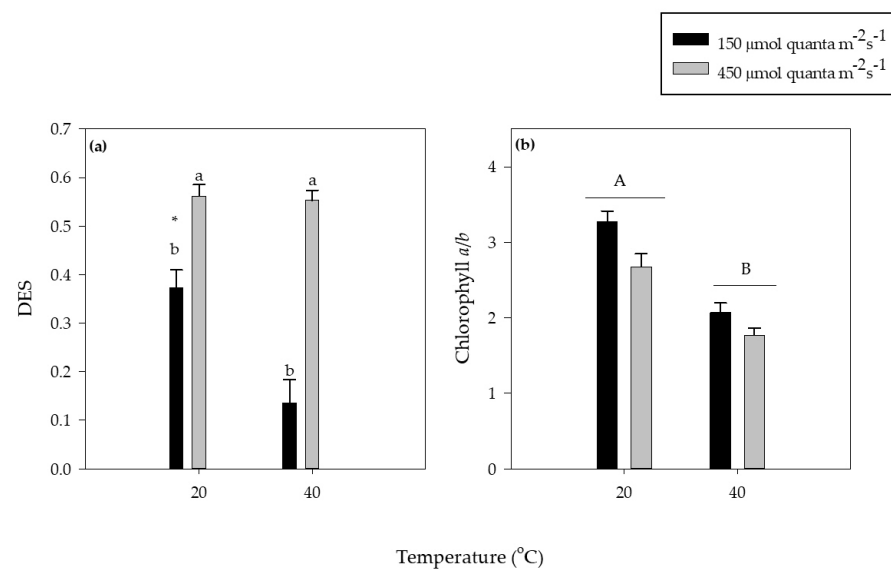


Figure 3. Effects of temperature and light on *Cymodocea nodosa*: (a) De-epoxidation ratio (DES) and (b) chlorophyll *a* to chlorophyll *b* ratio (Chlorophyll *a/b*). Values represent mean \pm SE ($n = 3$). Different letters indicate significant differences among light levels under the same temperature ($p < 0.05$, SNK test); * indicate significant differences among temperatures under the same light level ($p < 0.05$, SNK test); capital letters indicate differences among temperature independently of light level (no interaction among factors; $p < 0.05$, SNK test).

3.4. Soluble Sugars and Starch

There were no significant differences among soluble sugars concentrations in *C. nodosa* leaves submitted to irradiance and temperature treatments (Figure 4a). However, starch concentration in those leaves was almost twice higher at 40 °C than at 20 °C (Figure 4b). Light treatments did not influence starch concentrations.

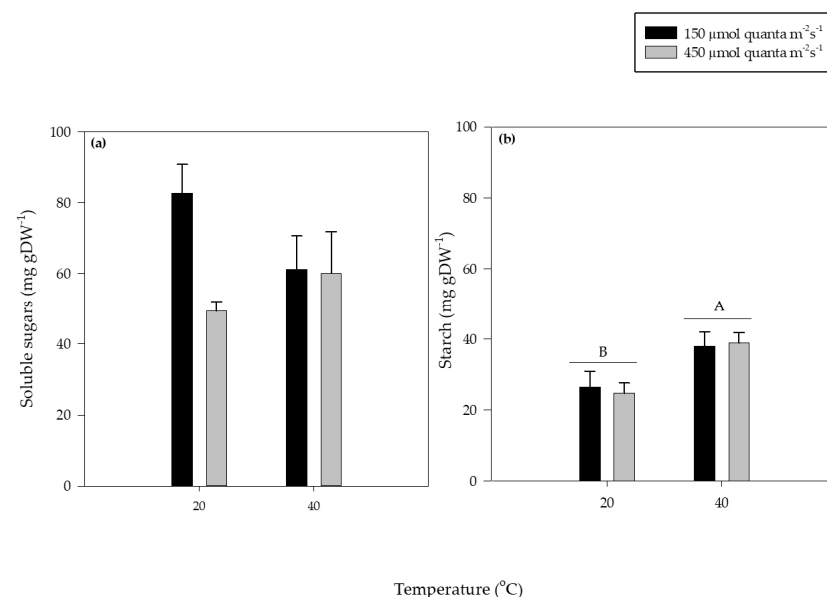


Figure 4. Effects of temperature and light on *Cymodocea nodosa*: (a) soluble sugars concentration and (b) starch concentration. Values represent mean \pm SE ($n = 3$). Different letters indicate significant differences among light levels under the same temperature ($p < 0.05$, SNK test); * indicate significant differences among temperatures under the same light level ($p < 0.05$, SNK test); capital letters indicate differences among temperature independently of light level (no interaction among factors; $p < 0.05$, SNK test).

4. Discussion

This work revealed that *Cymodocea nodosa* might show signs of stress under a heatwave of four days at 40 °C, as indicated by the increase in antioxidant response (TEAC and APX concentrations). These signs of stress were not aggravated by high light. There were also important changes in photosynthetic pigments as well as in photosynthetic and dark respiration processes. However, the species was able to tolerate well this experimental heatwave since no oxidative damage, measured by MDA, was detected.

Relevant changes of the relative concentrations of chlorophyll a, b, and carotenoids/chlorophyll ratio occurred at 40 °C. The decrease of the *C. nodosa* chlorophyll a/b ratio, also detected by other authors in other seagrass species submitted to heatwaves [51], suggests an unbalance between light harvesting and electron release into the electron transport chain, favoring the former and thus potentially leading to the overexcitation of chlorophyll a and the formation of chlorophyll triplets ($^3\text{Chl}^*$). Furthermore, the generalized decrease of carotenoids relative to chlorophyll unveils a waning capacity to dissipate excess energy, both in the reaction centers and light harvesting complexes. Both conditions favor the energy transfer from overexcited chlorophyll a to ground state O_2 generating singlet oxygen ($^1\text{O}_2$) and other reactive oxygen species (ROS) [52].

The de-epoxidation state of the pigments of the xanthophyll cycle (DES) typically increases with increasing light, especially when light intensity approaches photosynthetic saturation [53]. Zeaxanthin accumulation protects the photosynthetic antennae complexes by promoting the dissipation of excess excitation energy as heat and by quenching the chlorophyll triplet ($^3\text{Chl}^*$) and oxygen singlet ($^1\text{O}_2$) [54–56]. As expected, we also observed higher DES under high light (450 $\mu\text{mol quanta m}^{-2} \text{s}^{-1}$), driven by higher zeaxanthin concentration (Supplementary Materials Table S1), which indicates higher photoprotection capacity. The increase of DES under high light was followed by the decrease in the maximum quantum efficiency of PSII (F_v/F_m) and in the maximum photosynthetic rate (P_{max}), as expected, reflecting the increase of energy dissipation away from the PSII reaction centers [48].

The antioxidant response of *C. nodosa*, quantified by TEAC, was higher under the experimental heatwave, revealing processes of maintaining ROS concentrations below the level that causes cell damage [57], such as tocopherols, zeaxanthin, and carotenes, among others [58,59]. Tocopherols act together with VAZ-cycle to scavenge species as oxygen singlet under stressful situations [60,61]. The increased activity of *C. nodosa* APX under the heatwave is probably a response to the accumulation of H_2O_2 [62], which is an important signaling ROS molecule for stress acclimation [57,63,64]. APX removes excess H_2O_2 , preventing the formation of the highly destructive hydroxyl radical [65,66], thus decreasing or eliminating oxidative stress and the associated membrane lipid peroxidation. No signs of lipid peroxidation (measured with MDA) were observed in *C. nodosa*.

Despite the higher dark respiration rates induced by higher temperature, the foliar soluble sugar concentration was not affected, and the starch concentration increased, suggesting higher CO_2 assimilation. The increase of the effective quantum yield of photochemical energy conversion in PSII (ϕPSII) at 40 °C indicates higher electron transport [67] that may feed the Calvin cycle and potential sinks, such as photorespiration, the Mehler reaction (reduction of O_2 on the acceptor side of photosystem I), nitrogen and sulfur metabolism, and the export of reducing equivalents to mitochondria or peroxisomes [68]. Both photorespiration and the Mehler reaction are known producers of H_2O_2 and, although H_2O_2 produced in the peroxisomes by photorespiration is eliminated by catalase, the H_2O_2 that results from the Mehler reaction is scavenged by APX in the chloroplast [69]. The increase on APX activity we reported here may indicate an increase in the leaf production and scavenging of H_2O_2 and thus the redirection of excess electrons to the Mehler reaction. Additionally, the export of reducing equivalents to mitochondria, besides alleviating the reducing pressure next to photosystem I, would have resulted in higher O_2 consumption in the mitochondria, and may help to explain the increased dark respiration rates without affecting soluble sugar concentration.

No signs of lipid peroxidation were observed in *C. nodosa* under the experimental heatwave, as evidenced by the leaf MDA concentrations [42]. In fact, MDA was always within the values previously determined for non-stressed *C. nodosa* plants from the Ria Formosa (between ca 60 nmol g DW⁻¹ [28] and 140 nmol g DW⁻¹ (unpublished data)), and other non-stressed plants [70,71].

In conclusion, we showed here that *C. nodosa* could adjust its photophysiological processes and antioxidant defense mechanisms to successfully handle a short period of thermal stress. Light did not exert a synergistic effect with temperature and no oxidative damage was caused by the experimental heatwave. The positive response of *C. nodosa* to thermal stress draws a good perspective for its resilience under climate change scenarios, particularly when heatwaves are increasing in frequency and intensity, but further investigation, including successive heatwave events and recovery periods, is needed.

Supplementary Materials: The following is available online at <https://www.mdpi.com/article/10.3390/oceans2030025/s1>, Table S1: Effects of temperature (20 °C and 40 °C) and light (150 and 450 μmol quanta m⁻²s⁻¹) on *Cymodocea nodosa* photosynthetic pigments (μmol/gDw).

Author Contributions: Conceptualization, M.M.C., J.S., R.S., I.B.; methodology, M.M.C., I.B.; formal analysis, M.M.C.; investigation, M.M.C., R.S., I.B., J.S.; resources, R.S., J.S.; writing—original draft preparation, M.M.C.; writing—review and editing, M.M.C., J.S., I.B., R.S.; supervision, J.S., I.B., R.S.; funding acquisition, J.S., R.S. All authors have read and agreed to the published version of the manuscript.

Funding: This study received Portuguese national funds from FCT—Foundation for Science and Technology, through project UIDB/04326/2020, and is a contribution to the FCT project GrassMet (PTDC/MAR-EST/4257/2014). MMC was supported by Fundação para a Ciência e a Tecnologia PhD grant (SFRH/BD/64590/2009) from the Portuguese government.

Institutional Review Board Statement: Not applicable.

Informed Consent Statement: Not applicable.

Conflicts of Interest: The authors declare no conflict of interest.

References

- Waycott, M.; Duarte, C.M.; Carruthers, T.J.B.; Orth, R.J.; Dennison, W.C.; Olyarnik, S.; Calladine, A.; Fourqurean, J.W.; Heck, K.L.; Hughes, A.R.; et al. Accelerating loss of seagrasses across the globe threatens coastal ecosystems. *Proc. Natl. Acad. Sci. USA* **2009**, *106*, 12377–12381. [[CrossRef](#)]
- De los Santos, C.B.; Krause-Jensen, D.; Alcoverro, T.; Marbà, N.; Duarte, C.M.; van Katwijk, M.M.; Pérez, M.; Romero, J.; Sánchez-Lizaso, J.L.; Roca, G.; et al. Recent trend reversal for declining European seagrass meadows. *Nat. Commun.* **2019**, *10*, 1–8. [[CrossRef](#)]
- Sullivan, B.K.; Sherman, T.D.; Damare, V.S.; Lilje, O.; Gleason, F.H. Potential roles of *Labyrinthula* spp. in global seagrass population declines. *Fungal Ecol.* **2013**, *6*, 328–338. [[CrossRef](#)]
- Marbà, N.; Duarte, C.M. Mediterranean warming triggers seagrass (*Posidonia oceanica*) shoot mortality. *Glob. Chang. Biol.* **2009**, *16*, 2366–2375. [[CrossRef](#)]
- Arias-Ortiz, A.; Serrano, O.; Masqué, P.; Lavery, P.S.; Mueller, U.; Kendrick, G.A.; Rozaimi, M.; Esteban, A.; Fourqurean, J.W.; Marbà, N.; et al. A marine heatwave drives massive losses from the world's largest seagrass carbon stocks. *Nat. Clim. Chang.* **2018**, *8*, 338–344. [[CrossRef](#)]
- Collins, M.; Sutherland, M.; Bouwer, L.; Cheong, S.M.; Frölicher, T.; Des Combes, H.J.; Roxy, M.K.; Losada, I.; McInnes, K.; Ratter, B.; et al. Extremes, Abrupt Changes and Managing Risk. In *IPCC Special Report on the Ocean and Cryosphere in a Changing Climate*; Pörtner, H.-O., Roberts, D.C., Masson-Delmotte, V., Zhai, P., Tignor, M., Poloczanska, E., Mintenbeck, K., Alegria, A., Nicolai, M., Okem, A., et al., Eds.; Springer International Publishing AG: Cham, Switzerland, 2019.
- Kendrick, G.A.; Nowicki, R.J.; Olsen, Y.S.; Strydom, S.; Fraser, M.W.; Sinclair, E.A.; Statton, J.; Hovey, R.K.; Thomson, J.A.; Burkholder, D.A.; et al. A systematic review of how multiple stressors from an extreme event drove ecosystem-wide loss of resilience in an iconic seagrass community. *Front. Mar. Sci.* **2019**, *6*, 1–15. [[CrossRef](#)]
- Hobday, A.J.; Alexander, L.V.; Perkins, S.E.; Smale, D.A.; Straub, S.C.; Oliver, E.C.J.; Benthuisen, J.A.; Burrows, M.T.; Donat, M.G.; Feng, M.; et al. A hierarchical approach to defining marine heatwaves. *Prog. Oceanogr.* **2016**, *141*, 227–238. [[CrossRef](#)]
- Gao, K.; Beardall, J.; Häder, D.-P.; Hall-Spencer, J.M.; Gao, G.; Hutchins, D.A. Effects of ocean acidification on marine photosynthetic organisms under the concurrent influences of warming, UV radiation, and deoxygenation. *Front. Mar. Sci.* **2019**, *6*, 322. [[CrossRef](#)]

10. Campbell, S.J.; McKenzie, L.J.; Kerville, S.P. Photosynthetic responses of seven tropical seagrasses to elevated seawater temperature. *J. Exp. Mar. Biol. Ecol.* **2006**, *330*, 455–468. [[CrossRef](#)]
11. Pedersen, O.; Colmer, T.D.; Borum, J.; Zavala-Perez, A.; Kendrick, G.A. Heat stress of two tropical seagrass species during low tides—Impact on underwater net photosynthesis, dark respiration and diel in situ internal aeration. *New Phytol.* **2016**, *210*, 1207–1218. [[CrossRef](#)]
12. Marín-Guirao, L.; Ruiz, J.M.; Dattolo, E.; Garcia-Munoz, R.; Procaccini, G. Physiological and molecular evidence of differential short-term heat tolerance in Mediterranean seagrasses. *Sci. Rep.* **2016**, *6*, 28615. [[CrossRef](#)]
13. Rasmusson, L.M.; Lauritano, C.; Procaccini, G.; Gullström, M.; Buapet, P.; Björk, M. Respiratory oxygen consumption in the seagrass *Zostera marina* varies on a diel basis and is partly affected by light. *Mar. Biol.* **2017**, *164*, 140. [[CrossRef](#)]
14. De Silva, H.C.C.; Asaeda, T. Effects of heat stress on growth, photosynthetic pigments, oxidative damage and competitive capacity of three submerged macrophytes. *J. Plant Interactions* **2017**, *12*, 228–236. [[CrossRef](#)]
15. Olsen, Y.S.; Sánchez-Camacho, M.; Marbà, N.; Duarte, C.M. Mediterranean seagrass growth and demography responses to experimental warming. *Estuaries Coasts* **2012**, *35*, 1205–1213. [[CrossRef](#)]
16. Egea, L.G.; Jiménez-Ramos, R.; Hernández, I.; Brun, F.G. Effect of in situ short-term temperature increase on carbon metabolism and dissolved organic carbon (DOC) fluxes in a community dominated by the seagrass *Cymodocea nodosa*. *PLoS ONE* **2019**, *14*, e0210386. [[CrossRef](#)]
17. Chefaoui, R.M.; Duarte, C.M.; Serrão, E.A. Dramatic loss of seagrass habitat under projected climate change in the Mediterranean Sea. *Glob. Chang. Biol.* **2018**, *24*, 4919–4928. [[CrossRef](#)]
18. Savva, I.; Bennett, S.; Roca, G.; Jordà, G.; Marbà, N. Thermal tolerance of Mediterranean marine macrophytes: Vulnerability to global warming. *Ecol. Evol.* **2018**, *8*, 12032–12043. [[CrossRef](#)]
19. Koutalianou, M.; Orfanidis, S.; Katsaros, C. Effects of high temperature on the ultrastructure and microtubule organization of interphase and dividing cells of the seagrass *Cymodocea nodosa*. *Protoplasma* **2015**, *253*, 299–310. [[CrossRef](#)]
20. Yang, X.Q.; Zhang, Q.S.; Zhang, D.; Sheng, Z.T. Light intensity dependent photosynthetic electron transport in eelgrass (*Zostera marina* L.). *Plant Physiol. Biochem.* **2017**, *113*, 168–176. [[CrossRef](#)]
21. Ow, Y.X.; Uthicke, S.; Collier, C.J. Light levels affect carbon utilisation in tropical seagrass under ocean acidification. *PLoS ONE* **2016**, *11*, 1–18. [[CrossRef](#)]
22. Phandee, S.; Buapet, P. Photosynthetic and antioxidant responses of the tropical intertidal seagrasses *Halophila ovalis* and *Thalassia hemprichii* to moderate and high irradiances. *Bot. Mar.* **2018**, *61*, 247–256. [[CrossRef](#)]
23. Schubert, N.; Freitas, C.; Silva, A.; Costa, M.M.; Barrote, I.; Horta, P.A.; Rodrigues, A.C.; Santos, R.; Silva, J. Photoacclimation strategies in northeastern Atlantic seagrasses: Integrating responses across plant organizational levels. *Sci. Rep.* **2018**, *8*, 1–14. [[CrossRef](#)]
24. George, R.; Gullström, M.; Mangora, M.M.; Mtolera, M.S.P.; Björk, M. High midday temperature stress has stronger effects on biomass than on photosynthesis: A mesocosm experiment on four tropical seagrass species. *Ecol. Evol.* **2018**, *8*, 4508–4517. [[CrossRef](#)]
25. Kim, M.; Qin, L.Z.; Kim, S.H.; Song, H.J.; Kim, Y.K.; Lee, K.S. Influence of water temperature anomalies on the growth of *Zostera marina* plants held under high and low irradiance levels. *Estuaries Coasts* **2020**, *43*, 463–476. [[CrossRef](#)]
26. Silva, J.; Santos, R. Daily variation patterns in seagrass photosynthesis along a vertical gradient. *Mar. Ecol. Prog. Ser.* **2003**, *257*, 37–44. [[CrossRef](#)]
27. Yamori, W.; Hikosaka, K.; Way, D.A. Temperature response of photosynthesis in C3, C4, and CAM plants: Temperature acclimation and temperature adaptation. *Photosynth. Res.* **2014**, *119*, 101–117. [[CrossRef](#)]
28. Silva, J.; Barrote, I.; Costa, M.M.; Albano, S.; Santos, R. Physiological responses of *Zostera marina* and *Cymodocea nodosa* to light-limitation stress. *PLoS ONE* **2013**, *8*, e81058. [[CrossRef](#)]
29. Berry, J.; Bjorkman, O. Photosynthetic response and adaptation to temperature in higher plants. *Annu. Rev. Plant Physiol.* **1980**, *31*, 491–543. [[CrossRef](#)]
30. Devore, J.; Farnum, N. *Applied Statistics for Engineers and Scientists*; Brooks/Cole Publishing Company: Pacific Grove, CA, USA, 1999; p. 656.
31. Jassby, A.D.; Platt, T. Mathematical Formulation of the Relationship between Photosynthesis and Light for Phytoplankton. *Limnol. Oceanogr.* **1976**, *21*, 540–547. [[CrossRef](#)]
32. Enríquez, S.; Merino, M.; Iglesias-Prieto, R. Variations in the photosynthetic performance along the leaves of the tropical seagrass *Thalassia testudinum*. *Mar. Biol.* **2002**, *140*, 891–900. [[CrossRef](#)]
33. Costa, M.M.; Barrote, I.; Silva, J.; Olivé, I.; Alexandre, A.; Albano, S.; Santos, R. Epiphytes modulate *Posidonia oceanica* photosynthetic production, energetic balance, antioxidant mechanisms and oxidative damage. *Front. Mar. Sci.* **2015**, *2*, 111. [[CrossRef](#)]
34. Huang, D.; Ou, B.; Prior, R.L. The chemistry behind antioxidant capacity assays. *J. Agric. Food Chem.* **2005**, *53*, 1841–1856. [[CrossRef](#)]
35. Huang, D.; OU, B.; Hampsch-Woodill, M.; Flanagan, J.A.; Prior, R.L. High-throughput assay of oxygen radical absorbance capacity (ORAC) using a multichannel liquid handling system coupled with a microplate fluorescence reader in 96-well. *J. Agric. Food Chem.* **2002**, *50*, 4437–4444. [[CrossRef](#)]

36. Dudonné, S.; Vitrac, X.; Coutière, P.; Woillez, M.; Mérillon, J.M. Comparative study of antioxidant properties and total phenolic content of 30 plant extracts of industrial interest using DPPH, ABTS, FRAP, SOD, and ORAC assays. *J. Agric. Food Chem.* **2009**, *57*, 1768–1774. [[CrossRef](#)]
37. Sun, S.; Pan, S.; Ling, C.; Miao, A.; Pang, S.; Lai, Z.; Chen, D.; Zhao, C. Free radical scavenging abilities in vitro and antioxidant activities in vivo of black tea and its main polyphenols. *J. Med. Plants Res.* **2012**, *6*, 114–121. [[CrossRef](#)]
38. Re, R.; Pellegrini, N.; Proteggente, A.; Pannala, A.; Yang, M.; Rice-Evans, C. Antioxidant activity applying an improved ABTS radical cation decolorization assay. *Free Radic. Biol. Med.* **1999**, *26*, 1231–1237. [[CrossRef](#)]
39. Polle, A.; Pfirmann, T.; Chakrabarti, S.; Rennenberg, H. The effects of enhanced ozone and enhanced carbon dioxide concentrations on biomass, pigments and antioxidative enzymes in spruce needles (*Picea abies* L.). *Plant Cell Environ.* **1993**, *16*, 311–316. [[CrossRef](#)]
40. Polle, A.; Morawe, B. Properties of ascorbate-related enzymes in foliar extracts from beech (*Fagus sylvatica* L.). *Phyton* **1995**, *35*, 117–129.
41. Noctor, G.; Lelarge-Trouverie, C.; Mhamdi, A. The metabolomics of oxidative stress. *Phytochemistry* **2015**, *112*, 33–53. [[CrossRef](#)]
42. Hodges, D.M.; DeLong, J.M.; Forney, C.F.; Prange, R.K. Improving the thiobarbituric acid-reactive-substances assay for estimating lipid peroxidation in plant tissues containing anthocyanin and other interfering compounds. *Planta* **1999**, *207*, 604–611. [[CrossRef](#)]
43. Abadía, J.; Abadía, A. Iron and Plant Pigments. In *Iron Chelation in Plants and Soil Microorganisms*; Barton, L.L., Hemming, B., Eds.; Academic Press Inc.: New York, NY, USA, 1993; pp. 327–343.
44. Lichtenthaler, H.; Buschmann, C. Chlorophylls and Carotenoids: Measurement and Characterization by UV-VIS Spectroscopy. In *Current Protocols in Food Analytical Chemistry*; Wrolstad, R.E., Acree, T.E., Decker, E.A., Penner, M.H., Reid, D.S., Schwartz, S.J., Shoemaker, C.F., Smith, D.M., Sporns, P., Eds.; John Wiley and Sons Inc.: Hoboken, NJ, USA, 2001; pp. F341–F438.
45. Larbi, A.; Abadía, A.; Morales, F.; Abadía, J. Fe Resupply to Fe-deficient sugar beet plants leads to rapid changes in the violaxanthin cycle and other photosynthetic characteristics without significant de novo chlorophyll Synthesis. *Photosynth. Res.* **2004**, *79*, 59–69. [[CrossRef](#)]
46. De las Rivas, J.; Abadía, A.; Abadía, J. A new reversed phase-HPLC method resolving all major higher plant photosynthetic pigments. *Plant. Physiol.* **1989**, *91*, 190–192. [[CrossRef](#)]
47. Demmig-Adams, B.; Adams, W.W., III. The role of xanthophyll cycle carotenoids in the protection of photosynthesis. *Trends Plant Sci.* **1996**, *1*, 21–26. [[CrossRef](#)]
48. Adams, W., III; Zarter, C.; Mueh, C.; Amiard, V.; Demmig-Adams, B. Energy Dissipation and Photoinhibition: A Continuum of Photoprotection. In *Photoprotection, Photoinhibition, Gene Regulation and Environment, Advances in Photosynthesis and Respiration*; Springer: Amsterdam, The Netherlands, 2006; pp. 49–64.
49. Burke, M.K.; Dennison, W.C.; Moore, K.A. Non-structural carbohydrates reserves of eelgrass *Zostera marina*. *Mar. Ecol. Prog. Ser.* **1996**, *137*, 195–201. [[CrossRef](#)]
50. DuBois, M.; Gilles, K.A.; Hamilton, J.K.; Rebers, P.A.; Smith, F. Colorimetric method for determination of sugars and related substances. *Anal. Chem.* **1956**, *28*, 350–356. [[CrossRef](#)]
51. Nguyen, H.M.; Kim, M.; Ralph, P.J.; Marín-Guirao, L.; Pernice, M.; Procaccini, G. Stress Memory in Seagrasses: First Insight into the Effects of Thermal Priming and the Role of Epigenetic Modifications. *Front. Plant Sci.* **2020**, *11*, 1–18. [[CrossRef](#)]
52. Niyogi, K.K. Photoprotection revisited: Genetic and molecular approaches. *Annu. Rev. Plant Biol.* **1999**, *50*, 333–359. [[CrossRef](#)]
53. Jahns, P.; Latowski, D.; Strzalka, K. Mechanism and regulation of the violaxanthin cycle: The role of antenna proteins and membrane lipids. *Biochim. Biophys. Acta* **2009**, *1787*, 3–14. [[CrossRef](#)]
54. Gilmore, A.M.; Hazlett, T.; Govindjee. Xanthophyll cycle-dependent quenching of photosystem II chlorophyll a fluorescence: Formation of a quenching complex with a short fluorescence lifetime. *Proc. Natl. Acad. Sci. USA* **1995**, *92*, 2273–2277. [[CrossRef](#)]
55. Xu, C.-C.; Lin, R.-C.; Li, L.-B.; Kuang, T.Y. Increase in resistance to low temperature photoinhibition following ascorbate feeding is attributable to an enhanced xanthophyll cycle activity in rice (*Oryza sativa* L.) leaves. *Photosynthetica* **2000**, *38*, 221–226. [[CrossRef](#)]
56. Foyer, C.H. Reactive oxygen species, oxidative signalling and the regulation of photosynthesis. *Environ. Exp. Bot.* **2018**, *154*, 134–142. [[CrossRef](#)]
57. Mittler, R. Oxidative stress, antioxidants and stress tolerance. Review. *Trends Plant Sci.* **2002**, *7*, 405–410. [[CrossRef](#)]
58. Bohm, V.; Puspitasari-Nienaber, N.L.; Ferruzzi, M.G.; Schwartz, S.J. Trolox equivalent antioxidant capacity of different geometrical isomers of α -carotene, β -carotene, lycopene, and zeaxanthin. *J. Agric. Food Chem.* **2002**, *50*, 221–226. [[CrossRef](#)] [[PubMed](#)]
59. Zulueta, A.; Esteve, M.J.; Frígola, A. ORAC and TEAC assays comparison to measure the antioxidant capacity of food products. *Food Chem.* **2009**, *114*, 310–316. [[CrossRef](#)]
60. Pospíšil, P. Molecular mechanisms of production and scavenging of reactive oxygen species by photosystem II. *Biochim. Biophys. Acta Bioenerg.* **2012**, *1817*, 218–231. [[CrossRef](#)]
61. Krieger-Liszak, A.; Trebst, A. Tocopherol is the scavenger of singlet oxygen produced by the triplet states of chlorophyll in the PSII reaction centre. *J. Exp. Bot.* **2006**, *57*, 1677–1684. [[CrossRef](#)]
62. Morita, S.; Kaminaka, H.; Masumura, T.; Tanaka, K. Induction of rice cytosolic ascorbate peroxidase mRNA by oxidative stress; the involvement of hydrogen peroxide in oxidative stress signaling. *Plant Cell Physiol.* **1999**, *40*, 417–422. [[CrossRef](#)]
63. Larkindale, J.; Mishkind, M.; Vierling, E. Plants Responses to High Temperature. In *Plant Abiotic Stress*; Jenks, M.A., Hasegawa, P.M., Eds.; Blackwell Publishing, Ltd.: Hoboken, NJ, USA, 2005; pp. 100–144.

64. Kawamura, Y.; Uemura, M. Plant Low-Temperature Tolerance and its Cellular Mechanisms. In *Plant Abiotic Stress*; Jenks, M.A., Hasegawa, P.M., Eds.; John Wiley and Sons, Inc.: Hoboken, NJ, USA, 2014; pp. 109–132.
65. Betteridge, D.J. What is oxidative stress. *Metabolism* **2000**, *49*, 3–8. [[CrossRef](#)]
66. Foyer, C.H.; Shigeoka, S. Understanding oxidative stress and antioxidant functions to enhance photosynthesis. *Plant Physiol.* **2011**, *155*, 93–100. [[CrossRef](#)] [[PubMed](#)]
67. Maxwell, K.; Johnson, G.N. Chlorophyll fluorescence—A practical guide. *Exp. Bot.* **2000**, *51*, 659–668. [[CrossRef](#)]
68. Kalaji, H.M.; Bąba, W.; Gediga, K.; Goltsev, V.; Samborska, I.A.; Cetner, M.D.; Dimitrova, S.; Piszcz, U.; Bielecki, K.; Karmowska, K.; et al. Chlorophyll fluorescence as a tool for nutrient status identification in rapeseed plants. *Photosynth. Res.* **2018**, *136*, 329–343. [[CrossRef](#)]
69. Asada, K. Production and scavenging of reactive oxygen species in chloroplasts and their functions. *Plant Physiol.* **2006**, *141*, 391–396. [[CrossRef](#)] [[PubMed](#)]
70. Zhang, J.; Kirkham, M.B. Antioxidant responses to drought in sunflower and sorghum seedlings. *New Phytol.* **1996**, *132*, 361–373. [[CrossRef](#)] [[PubMed](#)]
71. Zlatev, Z.S.; Lidon, F.C.; Ramalho, J.C.; Yordanov, I.T. Comparison of resistance to drought of three bean cultivars. *Biol. Plant.* **2006**, *50*, 389–394. [[CrossRef](#)]